A Single-Aperture, Single-Pixel Reader for Optical Frequency Identification

Xiaozhe Fan, James Hidalgo, and Walter D. Leon-Salas
Purdue University
Indiana, USA
Email: fan115@purdue.edu

2021 IEEE International Symposium on Circuits and Systems (ISCAS) | 978-1-7281-9201-7/20/$31.00 ©2021 IEEE | DOI: 10.1109/ISCAS51556.2021.9401470

***Abstract*—This paper presents a single-aperture, single-pixel reader for communication with Optical Frequency Identification (OFID) tags. OFID tags use solar cells to transmit and receive information wirelessly as well as to harvest radiant energy. Due to its single-aperture architecture, the reader's optical system provides a shared optical path for reception and transmission. Also, physical alignment between the reader and an OFID tag is visually guided using the reader's emitted light, securing a robust data link as long as the OFID tag is illuminated. In this paper, a description of the reader's optical and electronic sub-systems are presented. The transmitter and receiver circuits are described in detail. The transmitter, built with a linear LED driver, achieves a power efficiency of nearly 87%. The receiver, featuring a third-order bandpass filter, reduces both low-frequency and high-frequency ambient noise. A prototype of the reader was fabricated and housed in a custom 3D-printed enclosure. Test results show that the reader is able to receive modulated luminescent signals from an OFID tag at a distance of 1 m and at a data rate of 3 kbps.**

***Index Terms*—optical frequency identification, reader, optical communications**

I. Introduction

The rapid deployment of Internet-of-Things (IoT) related technologies is expected to result in tens of billions of smart interconnected devices [1]. To scale up an IoT network without necessarily increasing its energy budget, low-power and even self-powered IoT devices are needed [2]. Most IoT networks use radio frequency (RF) technology for communication due to the hardware availability, low cost, long-range coverage, and readily-available technical resources [3]–[5]. However, RF bands, especially unlicensed bands, are expected to become increasingly congested as a result of increased number of wireless devices [6]. In addition to RF band scarcity, in applications such as smart dusts, where the antenna size is much smaller than the radio wavelength, the use of RF technology is challenging due to its low power efficiency at small sizes [7].

Optical wireless communication (OWC), a technology complementary to RF-based communications, has attracted significant interest because it extends connectivity to the optical spectrum tapping into very large unlicensed bands [8]. Other advantages of OWC include: 1) no interference with sensitive medical or navigation equipement; 2) high-degree of collimation possible with simple optical components (lenses and mirrors); 3) possible use of exisiting lighting infrastructures and 4) inherent security due to line of sight requirement [9].

Several efforts to develop high-speed wireless optical data links have been reported in the literature [8,10]–[12]. In these works, information is transmitted unidirectionally using complex sending/receiving modulation techniques that aim to improve the data throughput. Although it is possible to achieve bi-directional optical communications using two symmetric unidirectional data links [13], this symmetric solution is not feasible in most low-power IoT applications where devices are power-constrained. Inspired by backscatter modulation used in RFID systems, the *Retro-VLC* technique has been investigated for low-power visible light communications (VLC) applications [14]–[17]. The *Retro-VLC* system consists of a reader and several low-power VLC backscatters that modulate the reflected light using a mirror and liquid crystal display (LCD). The reader is basically a modified indoor light source with a few add-ons such as a photodetector and a power line communication system [17]. Therefore, in this approach the light from a reader is used for optical communication and illumination. Without the aid of optics (e.g., lenses), the reader only supports a communication range of few meters. The communication range is further constrained because the reader's output power has to match typical indoor illumination levels. Recently, a new concept dubbed Optical Frequency Identification (OFID), has been proposed in [18,19]. The OFID technique exploits the luminescent radiation emitted by solar cells to transmit information wirelessly. The solar cell is also used to receive information and to harvest energy. A portable dual-aperture OFID reader was introduced in [22]. A basic conceptual diagram of the dual aperture reader is shown in Fig. 1. Bi-directional communication with this type of reader is possible when an OFID tag is present in the overlapping regions between the transmit and receive paths. A drawback of this arrangement is that the communication region depends on the distance between the reader and the tag and the relative angle between these two apertures. Moreover, the two-aperture architecture imposes challenges in real-time physical alignment with the OFID device [18,19,27].

The contribution of this work is the design and characterization of a single-aperture reader that ensures that the transmission and reception paths are physically self aligned. This paper also presents a detailed description of the electronic system with an emphasis on the transmitter and receiver circuits. Experiments to evaluate the reader's performance were carried out and results are reported.

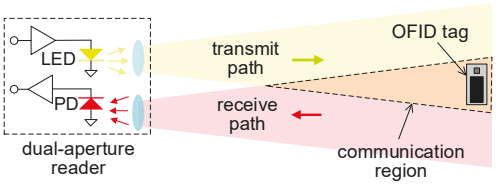

Fig. 1: Conceptual diagram of the dual-aperture OFID reader.

II. Preliminaries

As a new emerging communication concept, the OFID concept was first introduced in [18]. In this concept the luminescent emissions, both photo-luminescence (PL) and electro-luminescence (EL), of high-efficiency solar cells, such as GaAs solar cells, is exploited to transmit information [19]. A surprising result in solar cell research is that, in order to achieve high efficiency, solar cells must also be good light emitters [20]. GaAs solar cells, for instance, have strong luminescence in the near infrared (NIR) [21]. It has also been shown that there is an exponential relationship between luminescent intensity and the cell's terminal voltage with the PL intensity reaching its maximum and minimum when terminals of the cell are open or shorted, respectively [19]. Therefore, the PL emission of a solar cell can be modulated with binary information by alternatively opening and shorting the terminals of the solar cell as illustrated in Fig. 2(a). A conceptual diagram of an OFID communications system is shown in Fig. 2(b). The system consists of a reader or interrogating device and an OFID tag. The reader illuminates the solar cell in the tag to transfer energy and data by modulating its optical output power (downlink). The tag modulates the luminescence of its solar cell to transmit data back to the reader (uplink).

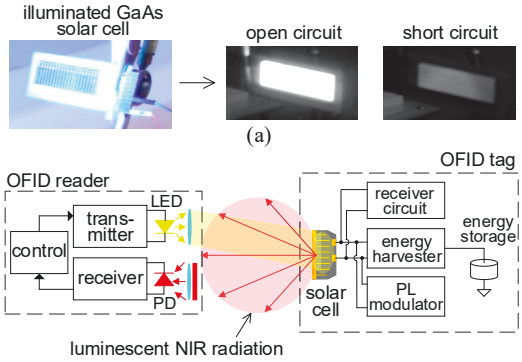

Fig. 2: Wireless optical communication with a solar cell. (a) A GaAs solar cell is illuminated with white LED light emits luminescent NIR radiation whose intensity changes by shorting and opening the solar cell's terminals. The images of the solar cell captured with a full-spectrum camera. (b) Conceptual diagram of an OFID communication system. A reader illuminates the solar cell in a tag stimulating a luminescent response that is modulated with data.

III. Reader Design

As shown in Fig. 3, the reader consists of two basic sub-systems: the optical sub-system and the electronic sub-system. The optical sub-system enables two-way point-to-point communications using a single optical aperture. In this design, light emitted by the reader not only conveys power and information and also aids to visually guide the reader's alignment with an OFID tag. The electronic sub-system interfaces with the optical sub-system through an LED and a single pixel or photodiode (PD). It performs the following tasks: modulation and demodulation, encoding and decoding, and data visualization. The rest of this section describes these two sub-systems in more detail.

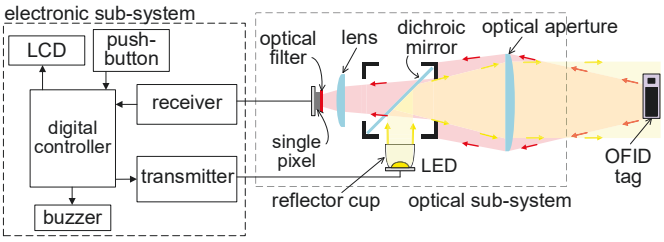

Fig. 3: Architecture of the proposed single-aperture, single-pixel OFID reader.

A. Optical Sub-System

We used a high-power LED that emits light at a peak emission wavelength of 620 nm (CREE XPEBRD-L1-0000-00902) for the downlink channel. A reflector (OPC OPC11COL) with a viewing angle of 7° is mounted on top of this LED to narrow the emitted light beam and minimize light leakage. A long-pass dichroic mirror (ThorLabs DMLP650), arranged at 45° with the LED axis, re-directs the LED light toward the OFID tag. This dichroic mirror, housed in a cage cube (ThorLabs CM1-DCH), has a reflectance of nearly 99.9% at the LED's emission wavelength. A plano-convex lens (ThorLabs LA1050), featuring a focal length of 100 mm and anti-reflection coating, is placed in between the dichroic mirror after the dichroic mirror and serves to collimate the light emitted by the reader. The PL radiation emitted by the GaAs solar cell in the OFID tag peaks in the near infrared (NIR) around 886 nm [19]. This PL radiation passes through both the plano-convex lens and the dichroic mirror. An aspheric lens, located between the dichroic mirror and the PD (Vishay Semiconductors BPW34S), focuses the incoming PL radiation onto the PD. An optical bandpass filter (Quanmin QM-NBF850-50) is mounted on top of the photodiode to remove undesirable optical interference.

B. Electronic Sub-System

The electronic sub-system includes the following components: transmitter, receiver, digital controller, and input/output devices such as a liquid crystal display (LCD), a push-button and a buzzer. The digital controller consists of a micro-controller unit (MCU), which together with the LCD, the push-button and the buzzer implements a basic user interface. The digital controller also includes a field programmable array (FPGA), which encodes transmitted signals and decodes received signals. Manchester codes are used for the encoding and decoding of signals. Fig. 4a shows the schematic diagram of the transmitter. The transmitter consists of a buck converter

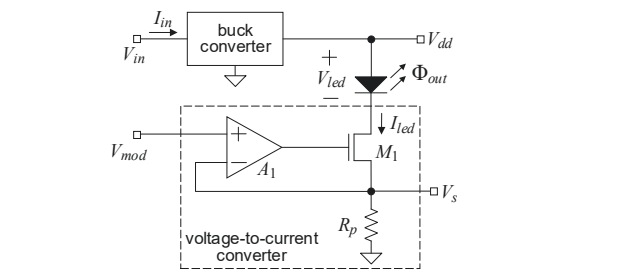

(a) transmitter

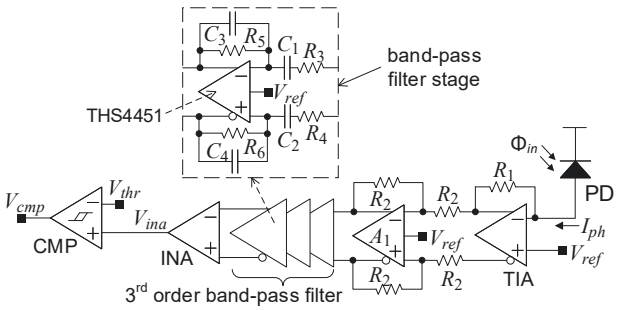

(b) receiver

Fig. 4: Schematic diagrams of the transmitter and receiver circuits.

and a voltage-to-current converter. The buck converter (Texas Instruments TPS54719) supplies the high current required by the LED. The operation amplifier A_1 (Analog Devices ADA4841) along with the NMOS M_1 (STMicroelectronics STL6N2VH5) form a feedback network that sets the LED's current I_{led} to:

$$I_{led} = \frac{V_{mod}}{R_p}. \tag{1}$$

Fig. 4b shows the schematic of receiver circuit. A PIN photodiode (Vishay Semiconductors BPW34) senses incoming optical signals and generates a photo-generated current I_{ph} proportional to the received radiant flux Φ_{in}.

$$I_{ph} = R_{pd}\Phi_{in} \tag{2}$$

where, R_{pd} is the spectral sensitivity and has units of A/W. A front-end trans-impedance amplifier (TIA) (Texas Instruments OPA857) amplifies I_{ph} with a trans-impedance gain of 20 kΩ (set by resistor R_1) and outputs a pseudo-differential voltage signal. The TIA is followed by the fully-differential amplifier A_1 (Texas Instruments THS4551) and a third-order band-pass filter. An instrumentation amplifier (INA) (Texas Instruments INA331) converts the fully-differential signal to a single-ended signal. Differential signalling was employed to minimize the effects of noise coupling. The comparator (CMP) (Texas Instruments LMV7239) compares the output of the INA, V_{ina}, with a threshold voltage V_{thr} and outputs a digital signal. The purpose of the band-pass filter is to remove DC ambient light interference, i.e. sun light, and low and high-frequency ambient noise from sources such as fluorescent lights. The filter has a -3 dB bandwidth of approximately 10 kHz, sufficient for receiving binary pulse-coded information at few kilo-bits per second [18]. The differential band-pass gain of the filter is 48 dB and the gain of the INA is set to 14 dB. The values of the passive components are set as follows: $R_2 = R_3 = R_4 = 15$ kΩ, $R_5 = R_6 = 75$ kΩ, $C_1 = C_2 = 47$ nF, $C_3 = C_4 = 110$ nF.

IV. Results and Discussions

As a proof-of-concept we built a prototype of the proposed single-aperture reader and tested it to verify its functionality. The first experiment we carried out sought to establish the output voltage of the buck converter in the transmitter circuit (V_{dd}) that results in the highest transmitter efficiency, η, in terms of power delivered to the LED over the input power, that is:

$$\eta = \left(\frac{V_{led} \times I_{led}}{V_{in} \times I_{in}}\right) \times 100\%. \tag{3}$$

Fig. 5 shows the efficiency η_{tot} as the current through the LED, I_{led}, is increased from 30 mA to 944 mA and for different values of the buck converter output V_{dd}. R_p was set to 0.23 Ω for this experiment and I_{led} was increased by increasing V_{mod}. Notably, as I_{led} increases, the efficiency also increases. However, the efficiency stops increasing when I_{led} becomes too large. This is because as V_{mod} increases, the drain-to-source voltage of M_1 in the voltage-to-current converter circuit decreases to the point where the feedback loop in the circuit can not longer regulate current.

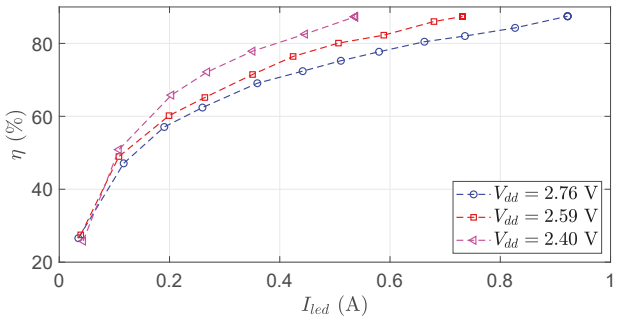

Fig. 5: Power efficiency η of the transmitter circuit as a function of the LED's forward current I_{led} and at different output voltages V_{dd} of the buck converter.

Fig. 6 shows the relationship between I_{led} and V_{mod} for $V_{dd} = 2.76$ V. The linear relationship between I_{led} and V_{mod} described in equation (1) can be appreciated. The figure also shows a linear modulation range for V_{mod} of 230 mV. Because of the linear relationship between I_{led} and V_{mod}, the transmitter circuit can be used to implement amplitude modulation schemes.

Another experiment evaluated the noise-filtering capability of the receiver circuit. Fig. 7 shows the normalized frequency response of the third-order bandpass filter. The -3 dB corner frequencies of the filter are 410 Hz and 10.7 kHz. For this experiment, the receiver was placed pointing to an office fluorescent light. The output of the INA, V_{ina}, was recorded

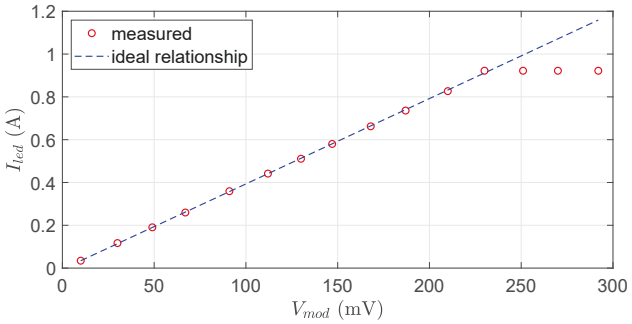

Fig. 6: Measured and ideal LED current I_{led} vs. modulation voltage V_{mod} for $R_p = 0.23\ \Omega$ and $V_{dd} = 2.76$ V.

with and without the filter. To remove the filter, capacitors C_1 and C_2 were shorted and capacitors C_3 and C_4 were removed. As shown in the figure, the spectrum of the fluorescent light exhibits peaks at 120 Hz, 39 kHz, 47 kHz, and 78 kHz. The figure also shows that the bandpass filter significantly attenuates interference. For instance, noise due to the fluorescent light decreases by 18 dB at 120 Hz and 31.38 dB at 39 kHz, respectively.

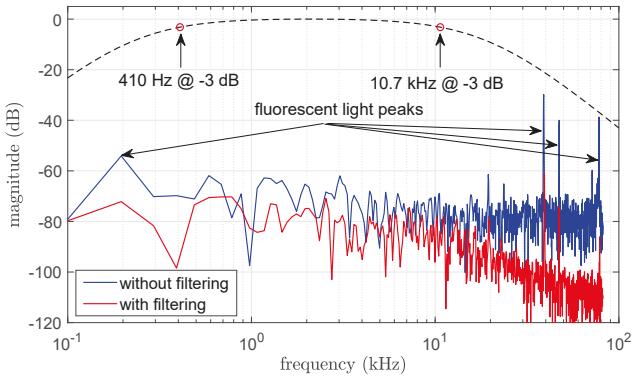

Fig. 7: Spectrum of the measured output of the INA with and without the third-order bandpass filter. The normalized frequency response of the bandpass filter (with 0 dB bandpass gain) is also plotted for comparison.

The last experiment validated the reader's functionality in receiving a modulated luminescence signal from an OFID tag. Fig. 8 shows a photograph and a diagram of the test setup. A simulated OFID tag was placed in front of the proposed reader at a distance of d = 1 m. The reader illuminated the OFID tag with an irradiance of 4.77 mW/cm^2 to stimulate the emission of luminescent radiation from the solar cell. The simulated OFID tag consists of a GaAs solar cell from Alta Devices, a MOSFET (M_1) and an FPGA. The FPGA generates a pseudo-random bit stream V_{dat} that drives the gate of M_1, shortening and opening the terminals of the solar cell, thus, modulating its luminescent emissions. V_{dat} was encoded using Manchester coding at a rate of 3 kbps to further mitigate the effect of ambient optical interference [25]. The reader, with both electronic and optical systems outfitted in a 3D-printed enclosure, received encoded photo-luminescent emission. Some critical signal waveforms were recorded using an oscilloscope, as shown in Fig. 9. As it can be seen, the received fully-digital signal V_{cmp}, matches very well with the transmitted signal V_{dat} in validating the proposed reader design.

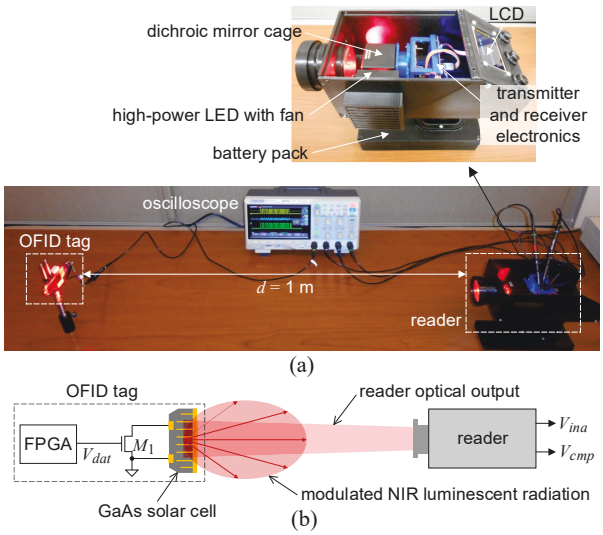

Fig. 8: Setup to test the the reader's operation. (a) photograph, (b) schematic diagram.

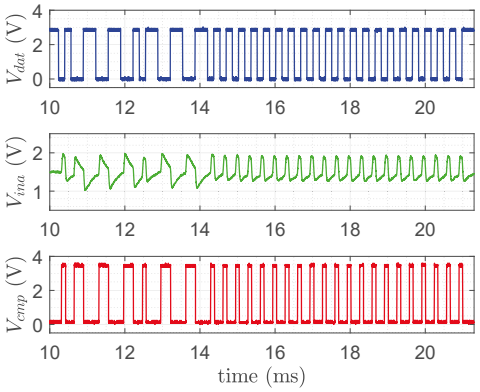

Fig. 9: Recorded waveforms during tag-to-reader communication test (V_{cmp} is inverted with respect to V_{dat}).

V. Conclusion

A single-aperture, single-pixel reader for OFID communications has been presented. The proposed reader has a shared optical path for both transmission and reception of information, easing the reader's alignment with an OFID tag. Both reader's optical and electronic systems were explained in detail. Several experiments were carried out to test and characterize the reader prototype. Experimental results validate the design. Future work will focus on improving the coupling effciency of both optical system.

Acknowledgment

The authors would like to thank the National Science Foundation for its support through grant ECCS 1809637.

REFERENCES

[1] S. Vashi, J. Ram, J. Modi, S. Verma and C. Prakash, "Internet of Things (IoT): a vision, architectural elements, and security issues," *International Conference on I-SMAC (IoT in Social, Mobile, Analytics and Cloud) (I-SMAC)*, Palladam, 2017, pp. 492-496.

[2] R. J. M. Vullers, R. V. Schaijk, H. J. Visser, J. Penders, and C. V. Hoof, "Energy harvesting for autonomous wireless sensor networks," *IEEE Solid-State Circuits Mag.*, vol. 2, no. 2, pp. 29–38, Jun. 2010.

[3] P. Kulkarni, Q. O. A. Hakim and A. Lakas, "Experimental Evaluation of a Campus-Deployed IoT Network Using LoRa," in *IEEE Sens. Jour.*, vol. 20, no. 5, pp. 2803-2811, 1 March1, 2020.

[4] X. Chen, Z. Li, Y. Chen and X. Wang, "Performance Analysis and Uplink Scheduling for QoS-Aware NB-IoT Networks in Mobile Computing," in *IEEE Access*, vol. 7, pp. 44404-44415, 2019.

[5] Q. Zhang, M. Jiang, Z. Feng, W. Li, W. Zhang and M. Pan, "IoT Enabled UAV: Network Architecture and Routing Algorithm," in *IEEE Internet of Things Journal*, vol. 6, no. 2, pp. 3727-3742, April 2019.

[6] J. I. d. O. Filho, A. Trichili, B. S. Ooi, M. Alouini and K. N. Salama, "Toward Self-Powered Internet of Underwater Things Devices," in *IEEE Comm. Mag.*, vol. 58, no. 1, pp. 68-73, January 2020.

[7] J. Liu, G. Faulkner, B. Choubey, S. Collins and D. C. O'Brien, "An Optical Transceiver Powered by On-Chip Solar Cells for IoT Smart Dusts With Optical Wireless Communications," in *IEEE Internet of Things Journal*, vol. 6, no. 2, pp. 3248-3256, April 2019.

[8] M. Z. Afgani, H. Haas, H. Elgala and D. Knipp, "Visible light communication using OFDM," *2nd International Conference on Testbeds and Research Infrastructures for the Development of Networks and Communities*, pp. 6, 2016.

[9] D. Tsonev, S. Videv, and H. Haas, "Towards a 100 Gb/s visible light wireless access network," *Opt. Express 23*, pp. 1627-1637, 2015.

[10] J. Fakidis, S. Videv, H. Helmers and H. Haas, "0.5-Gb/s OFDM-Based Laser Data and Power Transfer Using a GaAs Photovoltaic Cell," in *IEEE Photon. Tech. Let.*, vol. 30, no. 9, pp. 841-844, 1 May1, 2018.

[11] Z. Wang, D. Tsonev, S. Videv and H. Haas, "On the Design of a Solar-Panel Receiver for Optical Wireless Communications With Simultaneous Energy Harvesting," in *IEEE J. on Sel. Areas in Comm.*, vol. 33, no. 8, pp. 1612-1623, Aug. 2015.

[12] S. Zhang, D. Tsonev, S. Videv, S. Ghosh, G. A. Turnbull, I. D. W. Samuel, and H. Haas, "Organic solar cells as high-speed data detectors for visible light communication," *Optica*, vol. 2, no. 7, pp. 607-610, 2015.

[13] A. Al-Halafi and B. Shihada, "UHD Video Transmission Over Bidirectional Underwater Wireless Optical Communication," in *IEEE Photon. J.*, vol. 10, no. 2, pp. 1-14, April 2018

[14] D. N. Mansell, P. S. Durkin, G. N. Whitfield, and D. W. Morley, "Modulated-retroreflector based optical identification system," Dec. 10 2002, uS Patent 6,493,123.

[15] J. Chellam and R. K. Jeyachitra, "Energy-efficient bi-directional visible light communication using thin-film corner cube retroreflector for self-sustainable IoT," in *IET Opto.*, vol. 14, no. 5, pp. 223-233, 10 2020

[16] E. Rosenkrantz and S. Arnon,""Modulated retro reflector for VLC applications," in *SPIE Opti. Eng. + Appl. Inter. Soci. for Opt. and Photon.*, 2014.

[17] S. Shao, A. Khreishah and H. Elgala, "Pixelated VLC-Backscattering for Self-Charging Indoor IoT Devices," in *IEEE Photon. Tech. Let.*, vol. 29, no. 2, pp. 177-180, 15 Jan.15, 2017.

[18] W. D. Leon-Salas and X. Fan, "Exploiting Luminescence Emissions of Solar Cells for Optical Frequency Identification (OFID)," *2018 IEEE Inter. Symp. on Cir. and Sys. (ISCAS)*, Florence, 2018.

[19] W. D. Leon-Salas and X. Fan, "Solar Cell Photo-Luminescence Modulation for Optical Frequency Identification Devices," in *IEEE Trans. on Cir. and Sys. I: Regular Papers*, vol. 66, no. 5, pp. 1981-1992, May 2019.

[20] O. D. Miller, E. Yablonovitch and S. R. Kurtz, "Strong internal and external luminescence as solar cells approach the Schockley-Queisser limit," *IEEE Journal of Photovoltaics*, vol. 2, no. 3, pp. 303-311, 2012.

[21] J. M. Raguse and J. R. Sites, "Correlation of electroluminescence with open-circuit voltage from thin-flim CdTe solar cells," *IEEE Journal of Photovoltaics*, vol. 5, no. 4, pp. 1175-1178, 2015.

[22] X. Fan, S. Lee and W. D. Leon-Salas, "An Optical Wireless Temperature Sensor," *2019 IEEE SENSORS*, Montreal, QC, Canada, 2019.

[23] G. Mura and E. Miranda, "Analytical model for the I-V characteristics of fresh and degraded commercial LEDs," *2017 IEEE 24th Int. Sym. on the Phys. and Fail. Anal. of Inte. Cir. (IPFA)*, Chengdu, 2017, pp. 1-4.

[24] Texas Instruments, "2.95 V To 6 V Input, 7-A Synchronous Step Down Converter," TPS54719 datasheet, Jun. 2012 [Revised Feb. 2016].

[25] C. W. Chow, C. H. Yeh, Y. F. Liu and P. Y. Huang, "Mitigation of Optical Background Noise in Light-Emitting Diode (LED) Optical Wireless Communication Systems," in *IEEE Photo. J.*, vol. 5, no. 1, pp. 7900307-7900307, Feb. 2013.

[26] J. A. Veitch and S. L. McColl, "Modulation of fluorescent light: Flicker rate and light source effects on visual performance and visual comfort," *Lighting Res. Technol.*, vol. 27, no. 4, pp. 243–256, Dec. 1995.

[27] W. D. Leon-Salas, X. Fan, Y. Zhang and S. Kadirvelu, "Wireless Optical Communications with GaAs Solar Cells," *Frontiers in Optics*, pp. JTu4A83, 2019.